A biophysical analysis of mitochondrial movement: differences between transport in neuronal cell bodies versus processes

Babu Reddy Janakaloti Narayanareddy[1], **Suvi Vartiainen**[2,3], **Neema Hariri**[2], **Diane K. O'Dowd**[1,2,+], and **Steven P. Gross**[1,+]

[1]Department of Developmental and Cell Biology, University of California Irvine, Irvine, California-92697, USA [2]Department of Anatomy and Neurobiology, University of California Irvine, Irvine, California-92697, USA [3]Institute of Biosciences and Medical Technology, University of Tampere, Finland

Abstract

There is increasing interest in factors that can impede cargo transport by molecular motors inside the cell. While potentially relevant (1), the importance of cargo size and sub-cellular location have received relatively little attention. Here we address these questions taking advantage of the fact that mitochondria—a common cargo—in *Drosophila* neurons exhibit a wide distribution of sizes. In addition, the mitochondria can be genetically marked with GFP making it possible to visualize and compare their movement in the cell bodies and processes of living cells. Using total internal reflection (TIRF) microscopy coupled with particle tracking and analysis, we quantified transport properties of GFP positive mitochondria as a function of their size and location. In neuronal cell bodies we find little evidence for significant opposition to motion, consistent with a previous study on lipid droplets (2). However, in the processes we observe an inverse relationship between mitochondrial size and velocity and run distances. This can be ameliorated via hypotonic treatment to increase process size, suggesting that motor mediated movement is impeded in this more confined environment. Interestingly, we also observe local mitochondrial accumulations in processes but not in cell bodies. Such accumulations do not completely block transport, but do increase the probability of mitochondria-mitochondria interactions. They are thus particularly interesting in relation to mitochondrial exchange of elements.

Introduction

Correct transport of proteins and other vesicles in axonal and dendritic compartments is important for proper functioning of the nervous system. Many neurodegenerative conditions including amyotrophic lateral sclerosis (ALS) and Parkinson's disease (3–5) are linked to failures in axonal transport. Further, molecular motor based transport plays a critical role in healing of axonal injuries (6, 7), which would thus be impaired by poor transport. Overall regulation of cargo motion in neurons is still poorly understood, though for mitochondria,

Corresponding author: sgross@uci.edu, dkodowd@uci.edu.
+Co-senior authors.

part of the regulation involves the Miro and Milton proteins (8, 9). Mitochondrial positioning in processes is crucial, as they may locally buffer calcium transients (10), and also produce ATP needed for multiple cellular activities, including formation of de novo synapses during development, and continuous maintenance/remodeling of synapses in the adult nervous system. The architecture of axonal and dendritic processes in single neurons can be quite complex and some processes are only slightly wider than the larger cargos (such as mitochondria) that move through them. As they move through such compartments, cargos are frequently very close to the membranes bounding the process, which we hypothesize is likely to increase resistance to the cargos' motion. Further, the presence of these bounding membranes may make it difficult to push other objects out of the way, because they have nowhere to move. Thus, theoretical studies (11) suggest that cargos likely encounter varying levels of opposition, at least some of which depend on cargo size, with larger cargos subject to increased resistance to motion. Because Lis1 helps groups of dynein motors add forces productively(12), a study where Lis1 alteration particularly affected neuronal transport of large lysosomes (1) is consistent with such a size-dependent opposition hypothesis. How important are such effects? Do they contribute significantly to the overall properties of cargo transport? Our data shows that in neurons cultured from the *Drosophila* brain, in the cell body there is no correlation between mitochondrial size and motion, but in the restricted confines of the processes, movement of these organelles is size dependent.

Motion in the cell body is unaffected by mitochondria size

To evaluate transport of mitochondria in neurons from the Drosophila CNS, primary cultures were prepared from the brains of late-stage pupae. All pupae were heterozygous for UAS-mitoGFP and one of three GAL4 driver lines targeting mitoGFP expression to different populations of neurons. With the elav-GAL4 driver, >70% of the neurons had GFP + mitochondria, consistent with this being a pan-neuronal driver line. When using the GH298-GAL4 and GH146-GAL4 drivers, that are expressed in smaller subpopulations of neurons in the adult brain (13), GFP+ mitochondria were expressed in ~10% and <10 neurons respectively, in each culture. Imaging was carried out at 2–4 days *in vitro,* using objective-based TIRF microscopy. Moving mitochondria were tracked with ~10nm resolution (14). The run distances and velocities of mitochondria were determined from video tracks (Fig. 1A) of time lapse TIRF images (5fps) using the LVCorr software (14). There was no difference in any of the parameters measured between the three driver lines, so the data was pooled for the analysis presented. Neurons that contained abundant fluorescent mitochondria were chosen for analysis. The soma size ranged from 7–17 μm, with a mean of 10.2+/−0.56 (+/− SEM, n=21). In the cell body, 37.1+/− 3.03 % of the visible mitochondria were moving. Overall, the above data reflects measurements from 19 cells in 6 different cultures, sampled over 6 minute windows.

The mitochondria in the cell body and processes showed a wide distribution of sizes that ranged from 0.4 to 5.0 μm in length. To determine the effect of size on the transport properties of mitochondria, the population was divided into two groups: small (length<=1500 nm with a mean of 0.72+/−0.02 μm, cell bodies and 0.91+/−0.03 μm, processes); and large (length>1500 nm with a mean of 3.56+/−0.25μm, cell bodies and 2.4+/−0.07 μm, processes). For a discussion of the relationship between apparent fluorescent size

and actual size, see supplement. The velocity and run distances (total displacement of mitochondria between two consecutive pauses) were calculated for each group. The averages of velocities (Fig. 1B) and run lengths (Fig. 1C) of the small and large mitochondria in the cell body were independent of size. Importantly, the average velocity of approximately 800 nm/sec is typical of the unloaded velocity for both kinesin and dynein (12, 15). Thus, in the cell body, the effect of drag appears negligible. Similar cargo-size independent transport properties in cell bodies have recently been reported while studying the effect of lysosome diameters on their transport in mammalian (BS-C-1) cells (16).

Motion in processes depends on mitochondria size

Processes in neurons are frequently quite narrow, and in such environments cargo transport might face varying levels of impedance. The neuritic processes selected for analysis here contained easily detectable fluorescent mitochondria, and the image window was focused on the distal most 30 μm segment of the process. In our hands there was no significant difference in velocity, run-lengths or pause frequency of mitochondria moving in proximal (within 10μm of soma) versus distal locations in the processes (>25μm from soma) (Fig. S1. n=49 near and n=39 far). The average diameter of the neurites in which we tracked mitochondrial movement, determined from all of those for which we had DIC images, was 1.16+/− 0.1 μm (mean +/−SEM, N=19). Well above the diffraction limit of the point spread function (>400nm), the apparent and real sizes of the objects in differential interference contrast and fluorescent images are approximately equal with slight overestimation of the real sizes (~10%, Fig. S2 A&B). Recent theoretical calculations predict that when cargos are similar in size to the process diameter, the wall effects and macromolecular crowding play a large role in regulating transport (11). Thus, we experimentally characterized the effect of size on mitochondrial transport (N=46).

In this stage of culture, and without additional genetic markers, it was not possible to accurately identify axons vs dendrites, so we refer to these as 'processes'. We identified mitochondria as moving 'anterograde' or 'retrograde' when the location of the cell body could be definitively identified, but acknowledge that each group may include plus-end as well as minus-end directed transport. Ultimately, we found that motion was not statistically different in the two directions (see supplement), so in subsequent analysis anterograde and retrograde data was pooled. We find that mitochondrial transport in the processes is predominantly unidirectional, with occasional reversals. Overall, 44.2+/−4.6% of the visible mitochondria in the processes were mobile during the 10–20 minutes of continuous sampling. As in the cell body, there were more small mitochondria than large ones. Intriguingly, the average velocity and run-lengths of all mitochondria in the process were roughly half those of the averages in the cell body (Fig 1B and 1C). In addition, in contrast to the motion in the cell body, there is a significant inverse correlation between mitochondrion size and both velocity and run distance (Fig. 1B and 1C). Because motors under load (opposition to motion) slow down, and are more likely to detach from microtubules (17, 18), both observations suggest that mitochondria moving in the processes face significantly more opposition to motion than do those moving in the cell bodies. We observed occasional fission and fusion events but did not analyze those mitochondria that underwent fission or fusion during the recording time.

We briefly examined whether the distance from the cell body mattered for this effect (i.e. whether the effect was the same for motion in a portion of the process close to the cell body vs motion far away from the cell body), and found that the effect was approximately the same, regardless of distance from the cell body (see supplement).

We next analyzed motion as a function of mitochondrial size in more detail (Fig. 2), and found that for mitochondrial sizes below 1.5 microns, velocity and run-length were inversely correlated, but for mitochondria of 2 microns or larger, run-length and velocity were approximately constant. Interestingly, while the mean velocities of the smallest moving mitochondria are approximately 600 nm/sec, and approximately twice the means of the larger mitochondria, they have still not attained the presumably unloaded velocity of ~ 800 nm/sec measured in the cell body, suggesting that in the processes even the small mitochondria are under significant load.

Since our analysis suggests that larger mitochondria experience more opposition to motion in the processes (Fig 2A and 2B), we asked whether overall mitochondrial size might be chosen to decrease such opposition. Because our data suggests that the size cutoff for decreased opposition appears to be approximately 1.5 microns, we quantified the percentage of mitochondria 1.5 microns or less, finding it to be 71.2 % in the processes and 64.6% in the cell body. The overall high percentage of these smaller mitochondria is consistent with the hypothesis that their size might have been tuned to minimize opposition to motion. While further investigation will be useful, we note that in non-neuronal cells, mitochondria are typically larger (longer) (e.g. In Cos1 cells, we observe average mitochondrial lengths of 5 to 6 microns). It will be particularly interesting to investigate whether cells with larger caliber processes (where boundary effects will be less important) tend to have more mitochondria above this cutoff size.

Origin of the opposition to motion: the role of the bounding membrane

This study was motivated by the hypothesis that the presence of the membrane of the process would increase opposition to motion on cargos moving close to it, and that such opposition to motion would depend on cargo size. We tested this by treating the cultured neurons with a hypotonic solution (to induce swelling, and thus on average move the process membrane away from the mitochondria). Analysis of mitochondrial velocities and run-lengths under these conditions was consistent with our hypothesis: during exposure to hypotonic solution, the mean velocity and run-lengths of mitochondria was increased in the processes (Fig 1B & 1C, Fig 2), but not in the cell bodies (Fig. 1B and 1C).

The role of Actin

Actin might also play a role in mitochondrial motion, either promoting or opposing it. To test this, we used Latrunculin A (Santa Cruz Biotech, USA) to depolymerize actin, and again quantified velocities and travel distances in the cell body and processes. Depolymerizing actin had little effect on velocity or run-lengths in the cell body, but did increase each in the processes (Supplementary Movies 1 & 2); see discussion.

Increased pause time at mitochondria aggregates

Movement of each individual mitochondrion is not continuous, but is instead punctuated by frequent pauses, with an average pause duration of 7.5 seconds. In addition to moving mitochondria, the majority of the processes had at least one aggregate of stationary mitochondria in the 30 μm segment in which mitochondria movement was assessed (see e.g. two red stars, Fig. 3A & 3B first panel). Some aggregates were small (composed of 3–6 distinguishable mitochondria), whereas some were large and the mitochondria were tightly enough packed that by fluorescence microscopy individual mitochondria could no longer be distinguished. Consistent with a past report characterizing transport in mutant axons in the fly (19), individual mitochondria appear to pass through both kinds of aggregates. However, the average pause time of mitochondria when they encounter aggregates is approximately four times longer than the pause time of mitochondria moving in a region with no other mitochondria (within 2μm), when they paused (Fig. 3C).

Were the mitochondria that exited the aggregates the same that entered? In general, we believe so. We could usually follow individual mitochondria as they passed through the smaller aggregates; such events comprised 73 % of the 55 events involving the aggregates. In the remaining 27%, the aggregates were larger or organized in such a way that it was not possible to distinguish the mitochondrion once it entered the aggregate. In such cases two criteria suggested that the mitochondrion that exited the aggregate after a delay was the same one that had entered earlier. First, the size of the mitochondrion entering and exiting were typically the same, to within experimental error. Second, the probability that a mitochondrion would exit an aggregate was low unless one was observed entering (in a time window of 60 seconds, if none entered, the probability of one exiting was about 6%, i.e. 1 out 15 events).

A larger percentage of small versus large mitochondria are mobile in neurites

Finally we asked whether there was a correlation between mitochondrial size and the probability of moving. In the cell body, a similar percentage of the large and the small mitochondria were moving (Fig. 3D). In contrast, in the processes the percentage of small mitochondria that were moving was significantly higher than the percentage of large mitochondria. We hypothesize that this difference reflects one of the challenges of moving in processes: because the large mitochondria experience more opposition to motion in the processes, they are more likely to get stuck.

Discussion

This study was motivated by a theoretical analysis (11) suggesting that in neurons, motor mediated transport of cargos in small diameter neuronal processes would be more difficult than in the larger diameter cell body. The availability of *Drosophila* with genetically tagged fluorescent mitochondria makes this an attractive model in which to evaluate motor mediated transport. However, it is difficult to evaluate mitochondrial movement in neurons, particularly their axons, in the intact *Drosophila* brain using available imaging techniques. Therefore this study focused on mitochondrial movement in neurons dissociated from brains of late stage pupae. When grown in cell culture for 2–3 days the neurons regenerate

processes (20–22) and we find that GFP tagged mitochondria movement can be easily tracked in both the large diameter cell bodies and the small diameter neurites. While mitochondrial transport parameters have not been previously reported in the intact CNS, the rate of movement is likely to reflect that occurring *in vivo* based on an average velocity, 0.4–0.8 μm/sec, that is similar to the velocity reported in motor axons in segmental nerves of semi-intact 3rd instar *Drosophila* larvae (19). However, when our analysis considered mitochondria size, there was an inverse correlation between size and velocity in the processes for smaller mitochondria. The average run length in the cultured neurons (0.7–1.7 μm) is somewhat shorter than the average in larval motor neurons (1.8–3 μm). Additional studies will be necessary to determine if this is due to differences in cell type, stage of development, and/or culture versus *in vivo*.

Motors slow down (23) when experiencing load that is a significant portion of their stalling force, so we suggest that opposition to movement in the small processes can likely reach at least 2–3 pN (see supplement). In the processes of these *Drosophila* neurons—but not in the cell bodies of the same cells—mitochondrial size does indeed matter, with smaller mitochondria moving faster and further. Importantly, even the small mitochondria appear 'loaded down', and their velocities and run lengths are much lower than what is observed for all mitochondria moving in the cell body.

It is formally possible that these differences result from very tight differential regulation of the mitochondrial transport apparatus as a function of mitochondrial size and spatial location. Nonetheless, because two sets of perturbations—hypotonic treatment and actin depolymerization—dramatically decrease the difference between motion parameters in the cell body vs in the processes, we favor a simpler interpretation: in each case the transport machinery is the same, independent of mitochondrial size and location, and motion differences result from increased opposition to motion in the process.

What is the source of the opposition to motion in the process? Well-established physics suggests that it is difficult to move objects close to boundaries, both because of non-slip boundary conditions (and hence increased local effective viscosity) and also because in a confined space it is difficult to move extended objects out of the path of motion because they have nowhere to go. We favor this interpretation here, supported by the experimental observation that the hypotonic treatment to increase the process's caliber (and move the process membrane away from the mitochondria) did decrease apparent opposition to motion in the process but not cell body, as judged by increased travel velocities and run-lengths (Fig. 1 and 2) only in the processes.

How then should the alterations in motion due to actin depolymerization be interpreted? Loss of actin filaments improved transport in the processes consistent with a previous report studying role of actin filaments in axonal transport but had little effect in the cell bodies, suggesting that actin contributes to opposition to motion predominantly in the processes. Our favorite model is that in the process, the actin contributes to forming a cortex that the membrane attaches to; in the absence of such actin, the membrane is then freer to expand locally, and thus motion is less opposed.

Alternatively, myosin motors on the mitochondria might also grab on to actin filaments in the process, opposing microtubule-based transport, and providing drag. One interesting possibility is that much of the actin is not cross-linked to other actin filaments, and is thus dragged along by the moving mitochondria. In such a case, the drag provided by these filaments would be increased due to the presence of the bounding membrane. Because the magnitude of the hypotonic effect is approximately the same as that due to the actin depolymerization, we find this idea intriguing, and worthy of additional study.

Regardless of the causes, the overall differences in mitochondrial motion as a function of size are interesting because they suggest that at least in small-caliber processes, mitochondrial fragmentation can be used to significantly alter overall mitochondrial motion.

In addition to containing many moving mitochondria, the processes in the cultured neurons also contained both small and large mitochondrial aggregates. While some large aggregates of nonmoving mitochondria had been described in diseased neurons (24, 25), and they had occasionally been observed as present in wild-type processes as well (6, 7), they were more common than we expected, with typically at least one in any 30 μm segment chosen. Many such 'aggregates' were relatively small, consisting of 3–6 closely spaced unmoving mitochondria. Nonetheless, the presence of these aggregates altered the transport of other mitochondria moving in either the anterograde or retrograde direction. As previously reported in *Drosophila* motor neurons, the aggregates do not completely block movement of mitochondria (19), but we observe that in the cultured brain neurons, they significantly increase the pause time. Thus, in principle, the frequency of such aggregates could be used to tune the overall rate of mitochondrial transport. More likely, these long pauses of moving mitochondria when they encounter aggregates suggest increased opportunities for mitochondria-mitochondria interactions: there are reports of transient and permanent fusions of mitochondria (26) which are believed to be a way of regenerating aged mitochondria, and these exchanges and fusions are presumably enhanced by repeated slow contacts between mitochondria. Thus, these swellings where sustained mitochondria-mitochondria interactions occur could be important for promoting exchange of mitochondrial components, and ultimately mitochondrial health in the distal axons. It remains for future work to determine if indeed these swellings are useful, instead of harmful as has previously been assumed.

Materials and Methods

Fly lines

Pupae were obtained from mating of mito-GFP lines (Bloomington Stock Center #8442 or #8443) that express GFP with a mitochondrial import signal to one of three enhancer traps line to label mitochondria in different neuronal subpopulations: elav[C155]-GAL4, (Bloomington Stock Center #458), GAL4 broadly expressed in neurons throughout adult CNS; GH298-GAL4 (Bloomington Stock Center #37294), GAL4 expressed in adult neurons including local neurons (LNs) in the antennal lobe; and GH146-GAL4 (obtained from Luquin Luo Lab), GAL4 expression restricted primarily to projection neurons (PNs) in adult antennal lobe.

Cultures

Primary neuronal cultures were prepared from brains of late stage pupae as previously described (27, 28). Cultures were maintained in a humidified 5% CO_2 incubator at 22–24°C and imaging experiments were performed between 2 and 4 days in vitro (DIV).

Imaging

Movies of fluorescent mitochondria were recorded using objective based total internal reflection microscopy (TIRFM). TIRFM is built on Nikon TE200 inverted DIC microscope by using a high numerical aperture objective (Nikon 1.49 NA, 100X objective, 1.4 NA condenser). The cultured cells grown on special dishes have either genetically encoded GFP or stained with 10nM TMRM dye. The medium was exchanged to HBSS (Hepes-buffered salt solution, (in mM) 120 NaCl, 5.4 KCl, 1.8 $CaCl_2$, 0.8 $MgCl_2$, 15 glucose, 20 HEPES, 10 NaOH, and 0.001% phenol red, pH 7.2–7.4.) before imaging. Very low level of excitation light from 488nm Ti-Sapphire laser (Coherent Inc) is used for imaging and emitted light is collected using suitable notch filter to filter out the excitation laser from reaching the camera. An EMCCD camera from Photometrics (QuantEM 512SC) is used to grab and save the images on to the disc using Photometrics Micromanager Software. The images have a spatial resolution of 60nm/pixel (After 2.5X lens attachment in front of the camera) and were captured at 5 frames a second. To reduce the photo-toxicity and bleaching, the circularly polarized excitation laser was synchronized with the automated opening of shutter and its intensity kept minimum. While imaging with the optimized intensity level there was no considerable bleaching for upto10 minutes of acquisition. Before acquiring the fluorescence images the DIC images were also acquired after reducing the exposure time and EM gain of the camera to avoid the pixel intensity saturation. The diameter of the processes were estimated from the DIC images through further image analysis.

Actin depolymerization

The neuronal cells were treated with 1 μM, 5 μM and 10 μM Latrunculin A (Santa Cruz Biotechnology, sc-202691) in HBSS solution for 15 minutes at 25°C prior to imaging. The analysis was carried out on 1 μM and 5 μM only as the motion stopped in cells treated with 10 μM after about 15 minutes. In our hands, 1 μM Latrunculin A solution was sufficient to alter the morphology of Cos1 cells attached to coverslips from well spread out to round shapes, thus confirming its effectiveness in depolymerizing actin networks.

Hypotonic conditions

Hypotonic solution were prepared from HBSS. The osmolarity of HBSS is 250 mOsm. Hypotonic HBSS was prepared by adding distilled water to achieve an osmolarity of 200 mOsm. The treatment method for hypotonic solutions was similar to Latrunculin A treatment. The solution with 200 mOsm osmolality was exchanged with culturing medium 15 minutes prior to imaging. The mitochondrial morphology was affected in solutions with below 200 mOsm osmolality.

Video Tracking

Template matching method is used to generate the video tracks. Custom written labview based Lvcorr software is used to track the positions of the mitochondria in the processes. The template generation for shorter mitochondria is carried out by selecting the whole organelle. For larger ones, a portion of the leading end is considered as the template and Lvcorr program did well in generating the tracks of isolated mitochondria with this approach. The tracks were broken whenever a mitochondria passed through a docked mitochondria. In such cases the position of the mitochondria were scored by generating the intensity line profile of the passing mitochondria to join the broken tracks. During the linear motion/run, if the average displacement in four subsequent frames is less than 100nm that mitochondria was considered to be in pause state.

Length of the mitochondria was estimated by generating the intensity line profile of the straight mitochondria in 5 successive grey scale images/frames and calculating the average length using a custom written algorithm in lab view. A threshold of 10% of maximum intensity was selected to find the edges of the mitochondria. The images for estimating the length were chosen in such a way that the mitochondria remained straight and there was no deformation or defocusing of mitochondria in the images. The raw data used for the analysis is presented in the Fig. S4.

Supplementary Material

Refer to Web version on PubMed Central for supplementary material.

Acknowledgments

References

1. Yi JY, Ori-McKenney KM, McKenney RJ, Vershinin M, Gross SP, Vallee RB. High-resolution imaging reveals indirect coordination of opposite motors and a role for LIS1 in high-load axonal transport. The Journal of cell biology. 2011; 195(2):193–201. [PubMed: 22006948]

2. Shubeita GT, Tran SL, Xu J, Vershinin M, Cermelli S, Cotton SL, Welte MA, Gross SP. Consequences of motor copy number on the intracellular transport of kinesin-1-driven lipid droplets. Cell. 2008; 135(6):1098–1107. [PubMed: 19070579]

3. De Vos KJ, Grierson AJ, Ackerley S, Miller CC. Role of axonal transport in neurodegenerative diseases. Annual review of neuroscience. 2008; 31:151–173.

4. Wilson RJ. Towards a cure for dementia: the role of axonal transport in Alzheimer's disease. Science progress. 2008; 91(Pt 1):65–80. [PubMed: 18453283]

5. Hollenbeck PJ, Saxton WM. The axonal transport of mitochondria. Journal of cell science. 2005; 118(Pt 23):5411–5419. [PubMed: 16306220]

6. Curtis R, Tonra JR, Stark JL, Adryan KM, Park JS, Cliffer KD, Lindsay RM, DiStefano PS. Neuronal injury increases retrograde axonal transport of the neurotrophins to spinal sensory neurons and motor neurons via multiple receptor mechanisms. Molecular and cellular neurosciences. 1998; 12(3):105–118. [PubMed: 9790733]

7. Misgeld T, Kerschensteiner M, Bareyre FM, Burgess RW, Lichtman JW. Imaging axonal transport of mitochondria in vivo. Nat Methods. 2007; 4(7):559–561. [PubMed: 17558414]

8. Guo X, Macleod GT, Wellington A, Hu F, Panchumarthi S, Schoenfield M, Marin L, Charlton MP, Atwood HL, Zinsmaier KE. The GTPase dMiro is required for axonal transport of mitochondria to Drosophila synapses. Neuron. 2005; 47(3):379–393. [PubMed: 16055062]

9. Glater EE, Megeath LJ, Stowers RS, Schwarz TL. Axonal transport of mitochondria requires milton to recruit kinesin heavy chain and is light chain independent. The Journal of cell biology. 2006; 173(4):545–557. [PubMed: 16717129]

10. Murchison D, Griffith WH. Mitochondria buffer non-toxic calcium loads and release calcium through the mitochondrial permeability transition pore and sodium/calcium exchanger in rat basal forebrain neurons. Brain research. 2000; 854(1–2):139–151. [PubMed: 10784115]

11. Wortman JC, Shrestha UM, Barry DM, Garcia ML, Gross SP, Yu CC. Axonal Transport: How High Microtubule Density Can Compensate for Boundary Effects in Small-Caliber Axons. Biophysical journal. 2014; 106(4):813–823. [PubMed: 24559984]

12. McKenney RJ, Vershinin M, Kunwar A, Vallee RB, Gross SP. LIS1 and NudE induce a persistent dynein force-producing state. Cell. 2010; 141(2):304–314. [PubMed: 20403325]

13. Stocker RF, Heimbeck G, Gendre N, de Belle JS. Neuroblast ablation in Drosophila P[GAL4] lines reveals origins of olfactory interneurons. Journal of neurobiology. 1997; 32(5):443–456. [PubMed: 9110257]

14. Carter BC, Shubeita GT, Gross SP. Tracking single particles: a user-friendly quantitative evaluation. Physical biology. 2005; 2(1):60–72. [PubMed: 16204858]

15. Xu J, Reddy BJ, Anand P, Shu Z, Cermelli S, Mattson MK, Tripathy SK, Hoss MT, James NS, King SJ, Huang L, Bardwell L, Gross SP. Casein kinase 2 reverses tail-independent inactivation of kinesin-1. Nature communications. 2012; 3:754.

16. Bandyopadhyay D, Cyphersmith A, Zapata JA, Kim YJ, Payne CK. Lysosome Transport as a Function of Lysosome Diameter. PloS one. 2014; 9(1):e86847. [PubMed: 24497985]

17. Klumpp S, Lipowsky R. Cooperative cargo transport by several molecular motors. Proceedings of the National Academy of Sciences of the United States of America. 2005; 102(48):17284–17289. [PubMed: 16287974]

18. Kunwar A, Vershinin M, Xu J, Gross SP. Stepping, strain gating, and an unexpected force-velocity curve for multiple-motor-based transport. Curr Biol. 2008; 18(16):1173–1183. [PubMed: 18701289]

19. Pilling AD, Horiuchi D, Lively CM, Saxton WM. Kinesin-1 and Dynein are the primary motors for fast transport of mitochondria in Drosophila motor axons. Molecular biology of the cell. 2006; 17(4):2057–2068. [PubMed: 16467387]

20. Su H, O'Dowd DK. Fast synaptic currents in Drosophila mushroom body Kenyon cells are mediated by alpha-bungarotoxin-sensitive nicotinic acetylcholine receptors and picrotoxin-sensitive GABA receptors. The Journal of neuroscience: the official journal of the Society for Neuroscience. 2003; 23(27):9246–9253. [PubMed: 14534259]

21. Oh HW, Campusano JM, Hilgenberg LG, Sun X, Smith MA, O'Dowd DK. Ultrastructural analysis of chemical synapses and gap junctions between Drosophila brain neurons in culture. Developmental neurobiology. 2008; 68(3):281–294. [PubMed: 18044733]

22. Gu H, Jiang SA, Campusano JM, Iniguez J, Su H, Hoang AA, Lavian M, Sun X, O'Dowd DK. Cav2-type calcium channels encoded by cac regulate AP-independent neurotransmitter release at cholinergic synapses in adult Drosophila brain. Journal of neurophysiology. 2009; 101(1):42–53. [PubMed: 19004991]

23. Svoboda K, Block SM. Force and Velocity Measured for Single Kinesin Molecules. Cell. 1994; 77(5):773–784. [PubMed: 8205624]

24. Shidara Y, Hollenbeck PJ. Defects in mitochondrial axonal transport and membrane potential without increased reactive oxygen species production in a Drosophila model of Friedreich ataxia. The Journal of neuroscience: the official journal of the Society for Neuroscience. 2010; 30(34):11369–11378. [PubMed: 20739558]

25. Webster HD. Transient, focal accumulation of axonal mitochondria during the early stages of wallerian degeneration. The Journal of cell biology. 1962; 12:361–383. [PubMed: 14005486]

26. Liu XG, Weaver D, Shirihai O, Hajnoczky G. Mitochondrial 'kiss-and-run': interplay between mitochondrial motility and fusion-fission dynamics. Embo Journal. 2009; 28(20):3074–3089. [PubMed: 19745815]

27. Jiang SA, Campusano JM, Su H, O'Dowd DK. Drosophila mushroom body Kenyon cells generate spontaneous calcium transients mediated by PLTX-sensitive calcium channels. Journal of neurophysiology. 2005; 94(1):491–500. [PubMed: 15772240]

28. Sicaeros B, Campusano JM, O'Dowd DK. Primary neuronal cultures from the brains of late stage Drosophila pupae. Journal of visualized experiments: JoVE. 2007; (4):200. [PubMed: 18979004]

Synopsis

Is cargo transport affected by subcellular location? We quantify motion of different size mitochondria in neuronal cell bodies and processes, and discover that movement is different in these two regions. In cell bodies, mitochondria move relatively rapidly, and motion is size-independent. In contrast, both velocity and run distances are decreased in processes, and are inversely correlated with mitochondrial size. Decreasing confinement via hypotonic treatment improved transport in the processes, but not the cell body. Our data thus suggests that motor mediated transport is significantly impeded in the more confined environment of the processes.
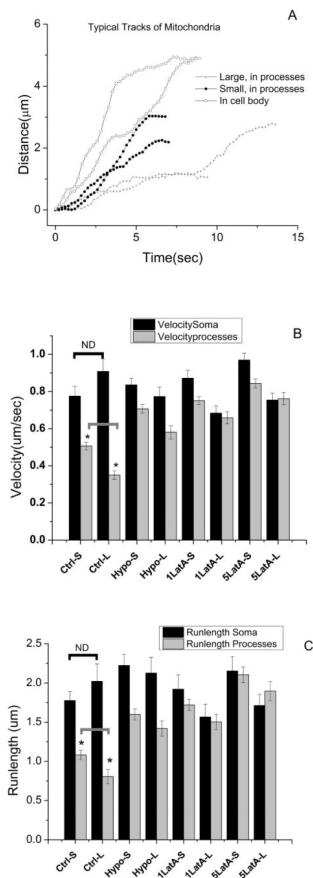
Fig. 1.
Transport parameters of mitochondria in neurons. A. Typical tracks of the mitochondria obtained from video tracking using Lvcorr software. Relationship between mitochondrial size and movement different in cell bodies versus processes. The differences in the velocity (B) and runlengths (C) of small (-S) and large (-L) mitochondria in the soma and processes observed in wild type neuronal cells is reduced when cultures are treated with hypotonic solution (osmolarity reduced from 250mOsm to 200 mOsm) and Latrunculin A (1 μM and 5 μM). * t-test, p<0.05 ND:Not significantly different.
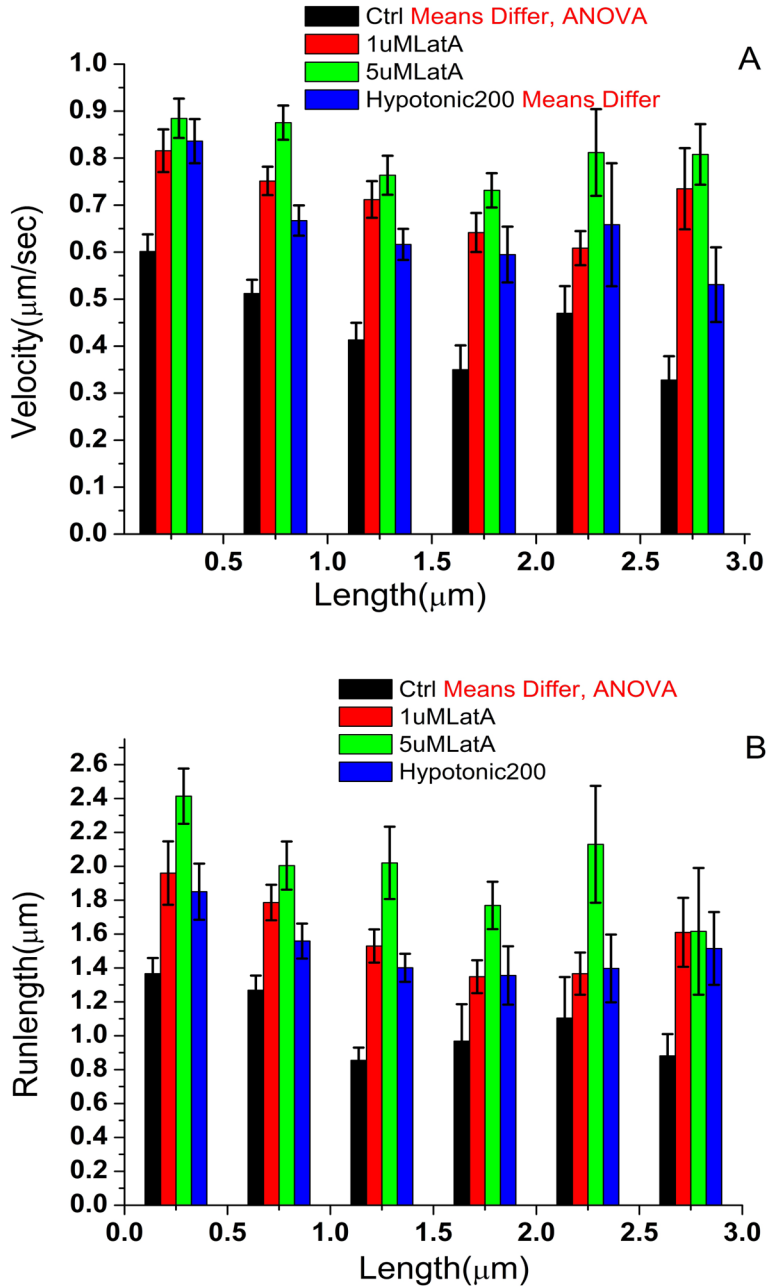
Fig. 2.
Mitochondrial velocities and run distances in the processes. A. Histograms of average mitochondrial velocity distributions as a function of their length in Ctrl, hypotonic and Latrunculin A treated cells. The velocities and run distances (B) are significantly longer for smaller mitochondria in control (Ctrl) cells. The differences are minimized with hypotonic or Latrunculin A treatment.
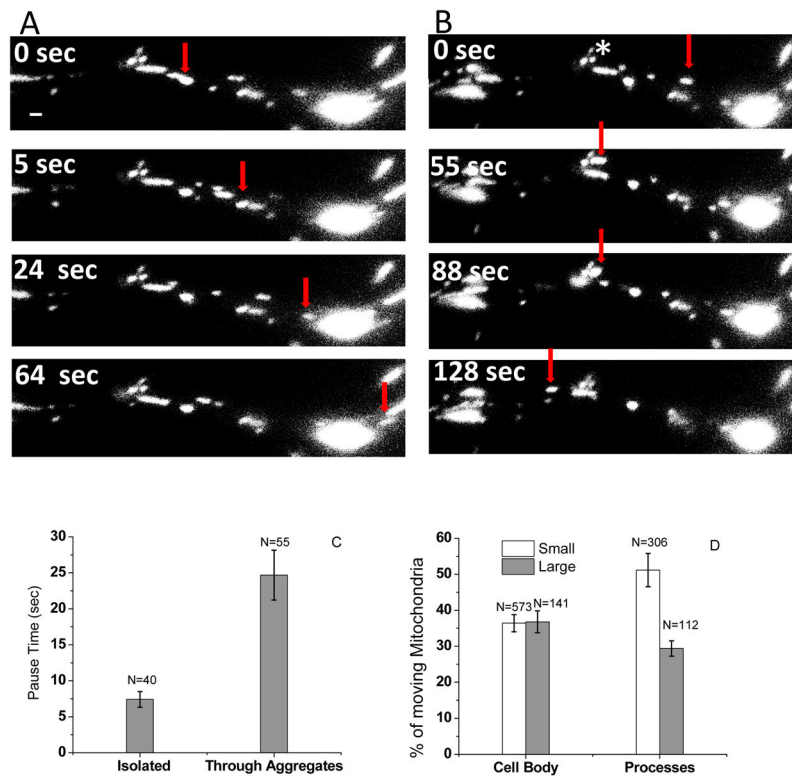
Fig. 3.
Longer pause times associated with mitochondrial aggregates in neurites. A & B. Typical
TIRF time lapse images with an individual mitochondrion indicated by red arrow it moves
through a large mitochondrial aggregate in the process. *Scale bar= 1 μm.* C. Average pause
time of mitochondria when they are isolated (separated by more than 2 μm from any other
mitochondria) is significantly shorter than when they encounter aggregates (7.36+/−1.63
sec, n=41 for isolated, 24.67+/−3.45, n=51 for aggregates). D. A similar percentage of small
and large mitochondria are moving in the cell bodies. In the processes the percentage
moving is significantly higher for the small versus the large mitochondria.